Interactive detection and visualization of breast lesions from dynamic contrast enhanced MRI volumes

Kalpathi R. Subramanian[a,*], John P. Brockway[b], William B. Carruthers[a]

[a]*Department of Computer Science, The University of North Carolina at Charlotte, Charlotte, NC 28223, USA*
[b]*Memory Testing Corp. and Novant Health, Charlotte, NC 28207, USA*

Abstract

Mammography is currently regarded as the most effective and widely used method for early detection of breast cancer, but recently its sensitivity in certain high risk cases has been less than desired. The use of Dynamic Contrast Enhanced Magnetic Resonance Imaging (DCE-MRI) has gained considerable attention in the past 10 years, especially for high risk cases, for smaller multi-focal lesions, or very sparsely distributed lesions. In this work, we present an interactive visualization system to identify, process, visualize and quantify lesions from DCE-MRI volumes. Our approach has the following key features: (1) we determine a *confidence* measure for each voxel, representing the probability that the voxel is part of the tumor, using a rough goodness-of-fit for the shape of the intensity-time curves, (2) our system takes advantage of low-cost, readily available *3D texture mapping hardware* to produce both 2D and 3D visualizations of the segmented MRI volume in *near real-time*, enabling improved spatial perception of the tumor location, shape, size, distribution, and other characteristics useful in staging and treatment courses, and (3) our system permits *interactive manipulation* of the signal–time curves, adapts to different tumor types and morphology, thus making it a powerful tool for radiologists/physicians to rapidly assess probable malignant volumes. We illustrate the application of our system with four case studies: invasive ductal cancer, benign fibroadenoma, ductal carcinoma in situ and lobular carcinoma.

© 2004 Published by Elsevier Ltd.

Keywords: Visualization; MRI; DCE-MRI; Confidence measure; Texture mapping; Volume rendering; Breast cancer; Ductal; Lobular; Detection

1. Introduction

X-ray mammography remains the most widely used radiological means to early detection of breast cancer. In conjunction with ultrasound, physical exam and needle biopsy, termed *triple assessment*, it is the current gold standard in clinical practice. On the other hand, its lower sensitivity to certain high risk cases has not been satisfactory [1,2]. Additionally, in cases of dense breast parenchyma or breast implants, X-ray mammography may be inconclusive or equivocal.

Magnetic resonance imaging (MRI) is a powerful imaging technique that has the ability to produce cross-sectional images of high spatial resolution at any orientation. It has the capacity to manipulate the contrast between different soft tissues. MRI can distinguish between soft tissues, based on magnetic-proton lattice interaction. These features have helped promote its wide clinical use, especially in producing accurate images of the central nervous system.

The use of MRI in breast imaging, termed MR mammography has gained considerable attention in recent years, especially for high risk cases [3]. Human breast tissue presents a challenge, however, as it is heterogeneous in the variability of tissues to be distinguished. Thus, the use of contrast agents, such as gadolinium-diethylenetriaminepentaacetic acid (Gd-DTPA), can increase the sensitivity of MRI. Dynamic contrast enhanced (DCE) MRI has been shown to help detect certain kinds of cancer cells in many

---

organs of the body such as the brain and lung. Two important factors have been suggested in enhancing tumor regions, (1) the effect of angiogenesis activity, resulting in increased vascularity (vessel density), and thus, increased contrast agent intake, and (2) increased vessel permeability, leading to increased *leakage* of contrast agent at the tumor site. Dynamic imaging of the breast (or a selected region of interest) makes it possible to functionally analyze the contrast intake and washout, using *signal–time* curves [4]. These factors can assist in improving the sensitivity and specificity of the lesions.

While direct visual examination of dynamic MR images continues to be the primary means to evaluate breast lesions, this is a laborious task; with increasing spatial and temporal resolution in the acquired MR volumes, manual processing and interpretation of dynamic MR volumes can quickly become infeasible. Additionally, there is considerable inter-observer and intra-observer variation in interpreting the enhancement of tumor regions [5]. Finally, variations in MRI techniques used at different sites, lack of consensus in architectural and kinetic features of tumors, differing morphologic and curve interpretation criteria have all motivated the development of breast imaging reporting and data system (BI-RADS) atlas [6], which provides a common language to report and compare breast tumor studies.

In this paper, our focus is on providing interactive visualization tools that provide physicians and radiologists the means to evaluate DCE-MRI volumes. We describe a new visualization and analysis system to process, detect and evaluate breast tumor lesions from DCE-MRI volumes. Using signal–time curve data at each voxel, we compute a *confidence* measure, representing the probability that it is, or is not malignant. The resulting *confidence volume*, in conjunction with the control volume (MRI volume without the contrast) is used to build a 3D texture. Using commodity graphics cards with 3D texture mapping hardware (for example, NVIDIA GE Force FX or ATI Radeon 9700), we use *texture mapped volume rendering* techniques to view and interact with the MR volume in *near real-time*. By suitably adjusting the transfer function, we can create semi-transparent renderings that display the lesions (single or multi-focal) distributed within the MR volume. Interactive viewing (rotation, panning and zooming) allows users to obtain a 3D perspective of the lesions, in terms of their location, shape, size, orientation and distribution. Inter-active manipulation and adjustment of the signal–time curves provides a powerful means to dealing with differing tumor characteristics. All of these features significantly reduce the efforts of radiologists in locating malignancies, and aid in standardizing curve characteristics from patient to patient.

We demonstrate our system on four breast tumor cases; invasive ductal cancer, benign fibroadenoma, ductal carcinoma in situ (DCIS) and lobular carcinoma.

2. Background

2.1. DCE-MRI

Advances in breast MR imaging are being driven by rapid changes in dedicated breast coils, protocol changes in MRI pulse sequences, and the use of contrast agents to enhance the appearance of lesions. Contrast agents, such as gadolinium-DTPA helps change (relaxation times) the magnetic state of hydrogen atoms in water molecules. This in turn results in marked enhancement in certain aspects of blood vessels. It is well understood that in the vicinity of a tumor, there is a higher probability of an increased supporting vasculature (due to its metabolic demand for oxygen) [7,8] of varying perfusion and levels of oxygenation, and a large blood volume. In T1-weighted images, these regions appear bright due to the increased intake of the contrast agent, while in gradient-echo T2-weighted images, the same regions appear darkened, indicating tissue perfusion.

In order to monitor intensity value of the contrast agent uptake (washin) and subsequent decrease in intensity (washout), the region of interest is imaged repeatedly, resulting in a *signal–time* function for each voxel within the entire tissue volume; an example is shown in Fig. 1. We suspect that analysis and interpretation of these signal–time curves will give us useful information on both the location and type of lesion, as described below. There is considerable variability world-wide by various researchers in the volume acquisition rate and the delay between acquisitions, with trade-offs between spatial and temporal resolution. The speed of acquisition depends on the size of the volume that is imaged, the strength of the magnetic field, the nature and number of channels of the dedicated coil, its type of phased array, and speed of its transceiver and transmitter.

2.2. Interpreting DCE-MRI images

In interpreting the signal–time curves resulting from DCE-MRI volumes, a three category classification is currently in use [4], as shown in Fig. 1. Curves are classified
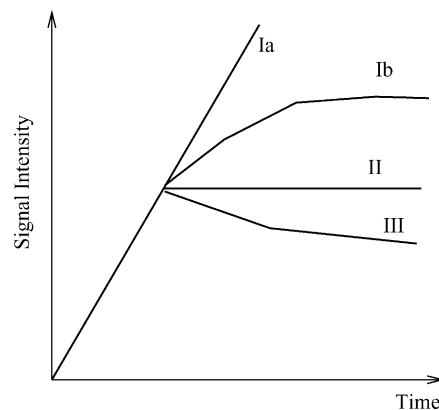

Fig. 1. Time–signal intensity curve types (reproduced from [4]).

as type I: steady enhancement (straight or curved), type II: plateau of signal intensity, and type III: washout of signal intensity. Types Ia and Ib have been suggested to be indicative of benign lesion, type II suggests possible malignancy, and type III strongly suggests malignancy. Kuhl et al. [4] found a strong correlation between benign and malignant lesions based on the shape of the signal–time intensity curve shape. Of the 266 cases studied, sensitivity of 91% and specificity of 83% was achieved, and an overall diagnostic accuracy of 86%.

This classification scheme, while providing a very valuable insight to identify and segment suspicious volumes, is subject to large physiologic variation. We suggest signal-intensity curve analysis provides a preliminary means to locate suspicious volumes within the breast, which can then be examined more carefully using additional metrics, such as location, shape and other morphological features.

A number of quantitative and estimation techniques have been proposed by researchers to interpret the signal–time curves, such as using the time delay between vessel and lesion enhancement [9], or using the percent enhancement beyond a certain time threshold. A second class of techniques focused on estimating the gadolinium concentration as a function of time, so as to extract pharmacokinetic parameters [10,11]. These kinetic curves may further be fit to empirical functions and parameters estimated for lesion classification, yielding a higher specificity. One disadvantage of these techniques is the high temporal resolution that is needed for maintaining accuracy, which in turn limits the size of the region being imaged. Overall accuracies of these techniques have considerable variance in terms of lesion sensitivity and specificity, and thus have not gained wide acceptance to date.

When there are multiple cancerous volumes, analyzing signal–time curves becomes tedious and error-prone, and requires examining individual voxels in image slices, depending on the tools available at a site. Even more complex, a single breast may contain more than one type of malignancy, adding complex variability to this inspection process. In our system, we have enabled interactive specification and modification of signal–time intensity curves followed by recalculation and display of cancerous sub-volumes over the entire breast volume. We suggest that near real-time volume visualization techniques for rapid analysis and quantification of breast lesions will increase radiologist hit rate and reduce error rates.

2.3. Texture mapped volume rendering

We use *volume visualization* techniques [12] to view and interact with the acquired DCE-MRI volumes. There are two broad approaches to rendering volumetric data, *surface based* techniques and *direct volume rendering* techniques. In surface based methods, the volume is transformed into surface primitives and then rendered as polygonal geometry.

A very popular method to generate surface primitives from volumetric data is Marching Cubes [13], where a specified contour surface (surfaces of a constant surface value) is algorithmically approximated and meshed into a set of triangular facets, and rendered using standard graphics engines. Direct volume rendering (DVR) techniques assume the volume is semi-transparent (each volume element has a specified opacity) and project the volume on to an image, by sampling the volume either front-to-back, as in the case ray-casting techniques [14], or back-to-front, as in compositing [15,16]; other DVR techniques include splatting [17], shear-warp factorization [18] and 3D texture mapping [19,20].

The biggest disadvantage of DVR techniques has been their computational expense, as they cannot take advantage of polygon rendering hardware. However, current graphics engines, such as Nvidia GEForce FX or the ATI Radeon, support real-time 3D *texture mapping*, which can be used to interactively view and manipulate the volume data. Moreover, by making the hardware more programmable at the geometry processing (vertex shaders [21]) and rasterization (fragment processing) stages [22], and the recent development of high level languages such as CG [23], texture mapped volume rendering has become an important means to render and manipulate volumetric data.

3D texture mapped volume rendering technique [19,20] consists of loading the 3D texture, which is the volume data. This is followed by generation of *proxy geometry*, typically a set of view-aligned polygonal slices, with the polygon vertices determining the texture coordinates. Volume rendering is accomplished by blending these slices in order [15,24]. This is efficiently performed in hardware, requiring resampling the volume data, as well as blending the slices in back-to-front or front-to-back order.

In our system, we use 3D texture mapped volume rendering to view DCE-MRI volumes, for two reasons, (1) 3D texture mapping hardware is readily available on low end computing platforms, and (2) texture mapped volume rendering permits real-time rendering and interactive manipulation of large volumes.

3. Methods

3.1. Data representation

A dataset consists of a 4D array of intensity values, interpreted as a sequence of volumes across time, or a single volume with multiple intensity components. For each voxel, a signal intensity-time curve can be plotted. This curve is used to determine the voxel's probability of being classified as malignant.

3.2. Volume visualization interface

The breast tumor visualization and analysis system we describe here was driven by the following considerations:

- An intuitive interface that allows easy access to information that is clinically useful for diagnosis and evaluation.
- A highly interactive interface that permits data exploration, allowing physicians/radiologists to influence the manner of data displayed, permitting optimal use of their cumulative expertise in evaluating breast tumor cases.
- Use of both 2D and 3D visualizations that is tightly coupled, permitting optimal understanding of tumor shape, size, location and morphology.

Fig. 3 shows a snapshot of the application interface. It consists of four major components, (1) 2D slice views, (2) 3D volume view, (3) signal–time intensity curve manipulation and confidence computation, and (4) tumor quantification. The curve manipulation interface is shown in the right panel of Fig. 3, and will be described later.

Three axis-aligned 2D views show orthogonal slices of the volume, corresponding to the axial, sagittal and coronal views. These axis-aligned slices are themselves extracted from the 3D texture volume. The 2D views can be interactively translated or scaled to focus on a particular region of the volume. Picking on any of the 2D views automatically updates the cross-hairs on the remaining 2D views, as well as the 3D view, so that the user maintains spatial context across all the views.

A single 3D perspective view shows a semi-transparent view of the entire volume, rendered using 3D texture mapping. The 3D view can be interactively translated or zoomed in/out. The 2D and 3D views are *linked* during interactive operations, so that the cursor position identifies the location in 3D space and simultaneously shows that same location in each of the three, 2D views. The user may select a single location within the 3D volume, represented by the three intersecting axes, or click to update the cross-hairs into any of the 2D slice views. Moving the cross-hairs in the 2D views updates the referenced location in the 3D volume view. However, direct picking in the 3D view is performed by locating the first probable cancerous location (high confidence region) along the picking ray, formed by the screen location and the viewing direction. 3D picking provides a convenient means to locate and select suspicious cancerous regions in the 3D view for closer examination, or to perform quantification. These regions are immediately updated in the three 2D views.

The 3D volume visualization in combination with real-time interaction provides spatial context to examining suspicious tumor lesions (their location, shape, size, etc.), while the 2D views permit more precise examination and a differing perspective within each slice. Linking the 2D and 3D views provides the 'bridge' to switch rapidly between the two views, allowing the user to localize and select a particular sub-volume. Hardware accelerated texture mapped volume rendering facilitates real-time viewing (panning, zooming and rotation) and interaction. In a typical scenario, a user would pick a suspicious lesion in the 3D view, which is immediately brought into the three 2D views (corresponding to the picked 3D point) for a closer examination. The real-time navigation capabilities of the volume view enables easy examination of 3D lesion shape, orientation and other morphological features. At the same time, the traditional means of examining consecutive axial, sagittal, and coronal slices (we use sliders) is retained. In these views, intensity values are mapped to shades of gray and cancerous regions are mapped to shades of red. In the 3D view, higher intensities and higher confidence values produce higher opacity (alpha) values.

3.3. Confidence measure computation

Our system computes a confidence measure for each voxel, representing the probability that it is part of a malignant lesion, thus requiring further analysis. Making this measure a continuous range avoids binary classification decisions which can result in aliasing errors, and helps quantify tumors more accurately. It also permits users to make multiple measurements for tumor volume by setting the confidence level (see Section 5).

To compute the confidence measure for a particular voxel, we can interactively specify a signal–time curve that roughly reflects the shape corresponding to the probable cancerous lesions in the dataset. Alternately, a user may pick a few voxels central to the lesion, and examine their signal–time curves. These can be selected and used to generate a *mean* curve shape. Each point on this mean curve (the small shaded squares in Fig. 2) is associated with an adjustable value range (min/max). All signal–time curves that fall within these ranges are assigned the maximum confidence value of 1.0 (the area between the dotted curves in Fig. 2). In addition two *threshold* curves are also specified; signal–time curves outside of the threshold curves are assigned a confidence value of 0.0. As shown in Fig. 2, the solid curve is the mean curve, while the dashed curves represent threshold curves. Voxels whose signal–time curves fall between
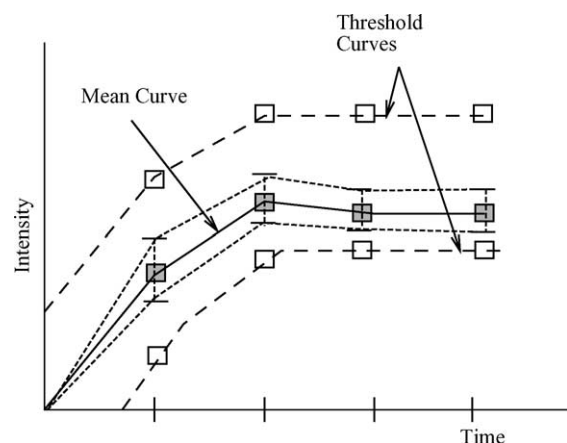

Fig. 2. Confidence measure computation.

the threshold curves and the dotted curves are assigned a confidence value between 0.0 and 1.0. We approximate this computation by evaluating the vertical distance of each sample point (transparent cube in Fig. 2) on the dashed curve to the closer dotted curve (we use five time steps in our experiments), and computing a value between 0.0 and 1.0, using linear interpolation. The product of these sample point 'confidence' values becomes the final confidence measure of the voxel.

3.4. Tumor quantification

The confidence volume described in Section 3.3 can be used to analyze and compute the volume of tumor lesions. This process begins by first selecting the lesion of interest, using 3D picking. Then a confidence threshold is specified; voxels with confidence values below this threshold are not considered to be part of the lesion. A connected component labeling algorithm is used to identify the voxels above the selected threshold. The lesion volume is then calculated by summing the volumes of the individual voxels, weighted by their associated confidence measure. Thus, holes or gaps within the lesion are not counted, and the weighted sum gives a more accurate volume measure, as the weight represents a probability.

Multiple lesions can be successively quantified; alternately our system permits the entire volume to be examined with connected component labeling, beginning from seed voxels having a confidence measure above a threshold (for instance, 0.9). These are stored in a list for later review.

4. Implementation

We have implemented our visualization system in C++ on PCs running Windows or Linux, and are equipped with an Nvidia GE Force FX5800 graphics card. Our graphical interface is built using the FLTK toolkit [25].

4.1. Rendering

Given a camera position and orientation, view-aligned slices are generated by intersecting a unit cube with a series of planes orthogonal to the view direction. As described earlier, the volume texture is mapped onto each of these slices, followed by blending these slices in front-to-back order. The three axis-aligned views are also extracted from the 3D texture, using texture lookups corresponding to each slice.

4.2. 3D texture/transfer function design

3D textures with RGBA (red, green, blue, alpha) components are generated by centering the MRI volume data within a 3D array. The red and green components of the texture are used to store intensity values (red representing

the MSB and green for the LSB). The blue component stores confidence values and the alpha value is currently unused. The user may specify which volume within the dataset provides intensity values. Before rendering, the entire texture is loaded into video memory.

Transfer functions provide the mapping from volume density values to color (RGB) and opacity (alpha), prior to slice compositing. Transfer functions can be as simple as a linear (or multi-ramps) mapping [15], or multi-dimensional [14,26–28]. In our current implementation, we represent transfer functions as Cg fragment shader programs [23], consisting of the following steps:

- A lookup is performed on the 3D texture using the interpolated 3D texture coordinate.
- The volume density is retrieved from the red and green components, interpreted as a 2 byte value. Because of current fragment shader limitations, values above 255 are truncated.
- Window and level parameters are applied to adjust the intensity.
- A pixel opacity value is computed using the blue component (from the computed confidence measure, as described earlier) and opacity parameter that represents the overall slice opacity.
- The output color is computed as (intensity + confidence) factor. Blue and green values are computed as (intensity − confidence) factor. This produces a bright red color in areas of high confidence and shades of gray in areas of low confidence.
- The output alpha value is set to the weighted sum of intensity and the confidence factor, multiplied by the opacity parameter. Different weights may be used for different transparency effects.

5. Experimental results

The interactive visualization system was tested on four DCE-MRI volumes, corresponding to invasive ductal cancer, benign fibroadenoma, DCIS and lobular carcinoma[1]. Table 1 describes the breast MRI protocols used. All of the data were acquired as part of an overall MR mammogram for women of high risk for breast cancer. These included women who had a history of breast cancer, familial breast cancer, carried the BRCA1 or BRCA2 gene, or were mammographically occult and ultrasonographically anomalous. In no case was there radiographic or ultrasonic data confirming suspicion of a lesion, with architectural distortion or conspicuous densities.

---

[1] Full resolution color images corresponding to these cases shown in Figs. 3–6 can be found at http://www.cs.uncc.edu/~krs/research.html.

Table 1
Breast MRI protocol

Series	Landmark	Image mode	Plane	Pulse sequence	VBW
3PL Loc	Xyphoid	2D	3-Plane	Localizer	Yes
Sag FSE T2	Sternal	3D	Sagittal	FSE-XL	Yes
T1 Special	Sternal	3D	Sagittal	SPGR	Yes
3D Gado.	Sternal	3D	Sagittal	SPGR	Yes

5.1. Case 1: Invasive Ductal Cancer

Case 1 (Fig. 3) shows a 39-year-old Caucasian female left breast, revealing two invasive ductal cancer regions. This was confirmed by fine needle aspiration biopsy.

Radiology assessment. Just lateral to the left nipple in the subareolar region is a heterogeneous nodular enhancing focus with irregular and nodular borders. The largest focal mass is on the order of 13–14 mm. Posterior and inferior to this are two adjacent nodules on the order of 5 mm each. These have enhancement profiles, increasing concern for multi-focal carcinoma in the left breast. There are other abnormal enhancing foci within the left breast, raising concern for distance disease. One is adjacent to the chest wall just lateral to the left nipple. This is deep within the parenchyma and is on the order of 3×5 mm. Another focus just inferior to the subareolar margin is on the order of 2–3 mm in size. There are three other tiny foci of enhancement superior to the largest tumor focus in the mid breast. These are present throughout and approximately 2 cm superior. These three tiny areas more superiorly are

indeterminate. Normal sized lymph nodes are present in the left axilla, although not well seen on this exam. This exam is suspicious for multi-focal, multi-quadrant disease.

Highly probable malignant appearing areas, similar to invasive lobular carcinoma characteristics.

5.2. Case 2: Normal Parenchymal Tissue

Case 2 (Fig. 4) shows a 58-year-old female with the contralateral left breast examined following right breast mastectomy. It is negative for cancer, and shows no false positives for benign fibroadenoma, although benign fibroadenoma is present in parenchyma anterior to the reconstructive implant.

Radiology assessment. Two circumferential small areas of enhancement are present in the upper and upper inner portions of the left breast with central areas of low signal intensity on all imaging sequences and are observed. These areas of halo-like enhancement are less than 10 mm in diameter and would probably not be palpable. No masses are detected. There is no evidence for spiculation or segmental type enhancement. Benign appearing fibroglandular enhancement is noted in the upper outer portion of the breast.

One focus/false blood vessel is detected: there is a submuscular silicon implant in place. No lymphadenopathy is detected. No skin or chest wall abnormalities are detected. There are two circumferential small areas of enhancement present in the upper and upper inner portions. These are not suspicious for malignancy.
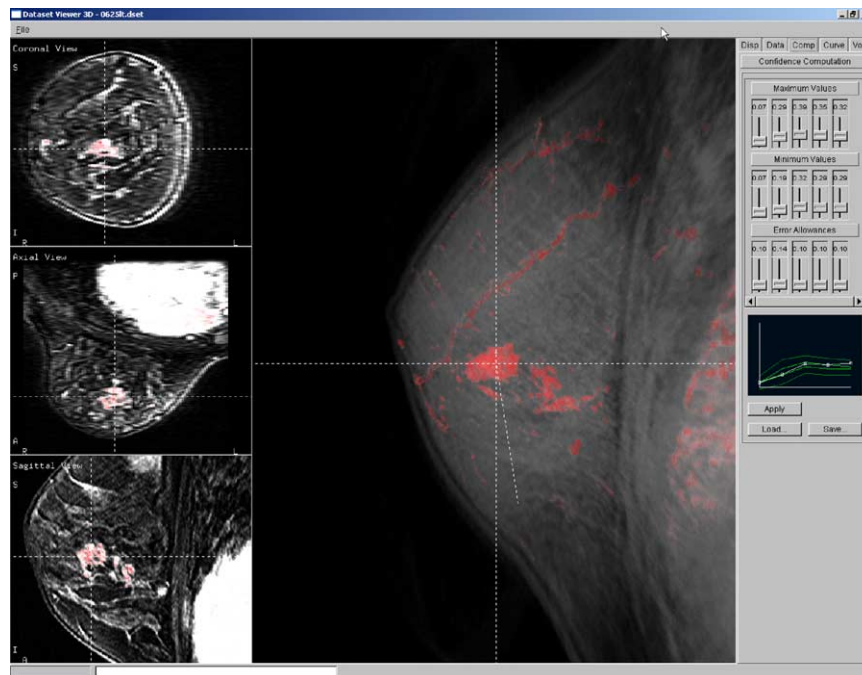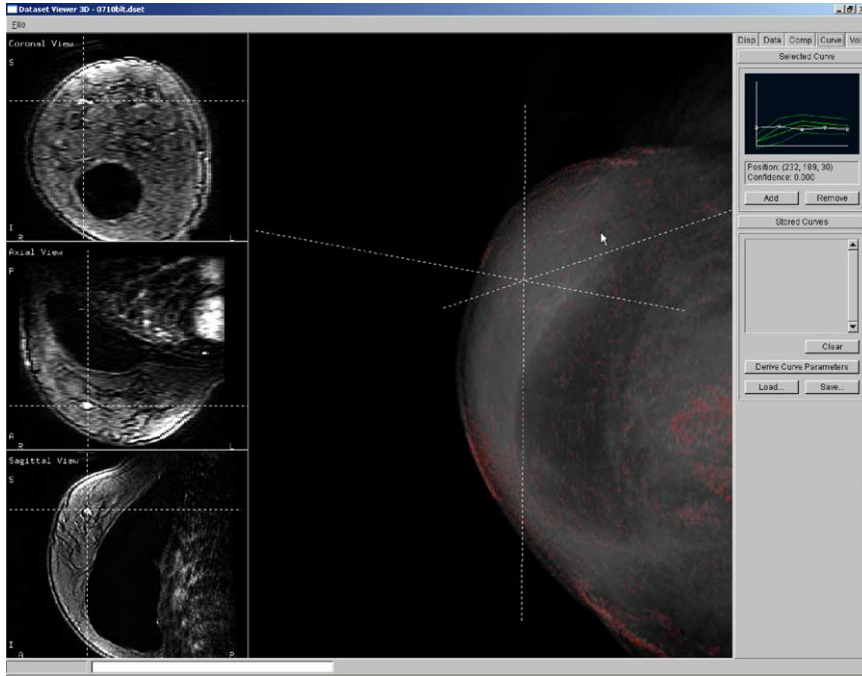

Fig. 3. Invasive ductal cancer.

Fig. 4. Benign fibroadenoma.

5.3. Case 3: Ductal Carcinoma In Situ (DCIS)

Case 3 (Fig. 5) shows a 39-year-old Caucasian female left breast with invasive ductal carcinoma with extensive DCIS; DCIS measures at least 5.6 cm with intermediate to high nuclear grade, solid and cribriform, with central necrosis.

Radiology assessment. In the left lower breast, there is a 3 cm seroma present in the prior biopsy site. Inferior to the seroma at the 6 o'clock position extending in the outer lower portion of the left breast, 5–4 o'clock position near the chest wall, there is an abnormal regional enhancement present. This is highly suspicious for residual malignancy extending over 3 cm in diameter. Diffuse non-malignant like enhancement is present throughout the remainder of the left breast. No definite masses are detected in the upper breast. No lymphadenopathy is detected. No skin nipple or chest wall involvement is detected.
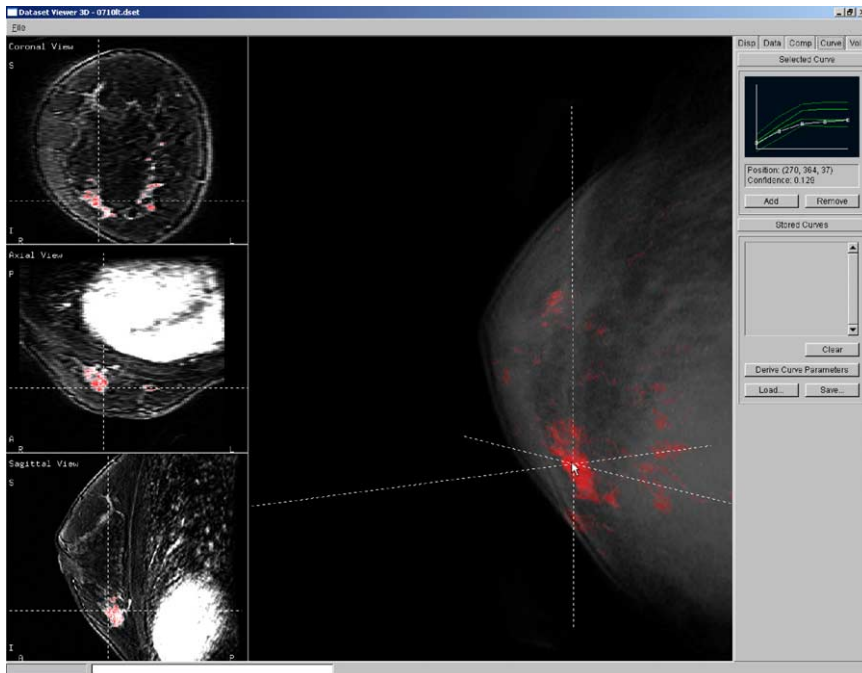

Fig. 5. Ductal carcinoma in situ (DCIS) and two areas of invasive ductal cancer.
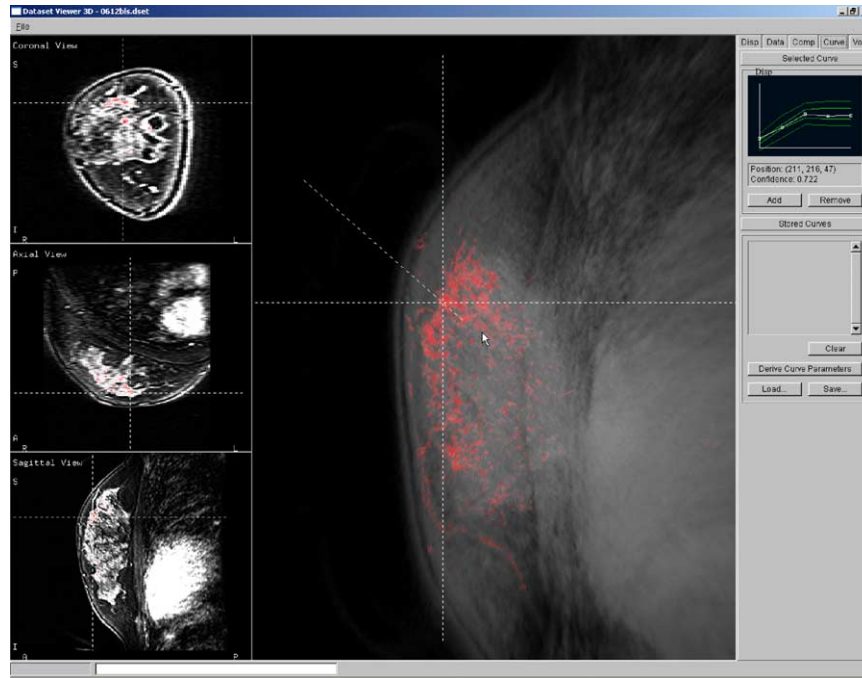
Fig. 6. Lobular carcinoma.

Left invasive DCIS with multi-focal malignancy with at least seven distinct volumes of disparate highly probable malignant looking regions ranging from 0.02 to 6.8 cm^3.

This case is highly suspicious for malignancy in the outer lower region of the left breast.

5.4. Case 4: Lobular Carcinoma

Case 4 (Fig. 6) shows a 53-year-old Caucasian female left breast with extensive lobular carcinoma with extension into the ducts extending into much of the breast among dense fibroglandular parenchymal tissue.

Radiology assessment. This case shows a clean left breast, no cancer, except for fibrocystic disease. Numerous small, scattered, benign cysts are interspersed among dense fibroglandular tissue. The DCE sequence shows diffuse, uniform enhancement of the dense fibroglandular tissue throughout the left breast but no focal contrast aberrations are identified and the contrast enhancement slope is characteristically benign throughout the fibroglandular tissue. No masses are recognized, and no architectural distortions or alterations or other suspicious features are observed.

Thus, in this case, the radiological assessment differed markedly, as visual inspection of diffuse malignancy is often easily overlooked. No architectural distortion can be observed. We depend heavily on computation of the confidence based on time–signal intensity curves to indicated malignancy, rather than visual inspection. Histology confirmed that the patient had lobular cancer, which was confirmed following lumpectomy and pathological workup.

6. Conclusions

In this work, we have taken the first step in providing interactive visualization tools for assessing breast lesions from DCE-MRI volumes. The focus is on providing an interactive exploratory system that eases the task of the radiologist in understanding time-varying volume datasets. Our system provides the capability to perform an automatic exhaustive search of the 3D volume for suspicious tumor lesions. At the same time, it provides the needed interactive tools that complements the expertise of the radiologist. This has the potential to increase the radiologist's hit rate and reduce errors.

Our system has the following important advantages:

- By allowing easy manipulation of the signal–time curves, the radiologists can utilize their expertise in looking for specific tumor types, for instance, using prior knowledge of the case under consideration.
- The visualizations consists of both 2D. and 3D views: 3D views provide better characterization of shape and size, while the traditional 2D views provide more precise information about lesions in specific parts of the volume.
- Linking the 2D and 3D views allows switching between the views without losing spatial context, as well as facilitate seamless and continuous navigation.

- Our approach to using a confidence measure provides a probability measure that is easily adjustable and also provides an accurate means of computing tumor volumes.

We tested our system on four breast tumor cases: invasive ductal cancer, benign fibroadenoma, DCIS and lobular carcinoma. Our system was in agreement with the first three cases. In the fourth case, our tool's assessment differed from the radiological assessment (false negative). Histology confirmed our tool's assessment, as well as pathological workup after lumpectomy.

There are several aspects of the visualization system that are ripe for improvement. The 3D views lack orientation information, as we are simply compositing the slices in order. We are in the process of incorporating gradient based shading to our volume renderer [22], which will improve the spatial perception of the tumor lesions. Secondly, we are exploring custom transfer functions to better segment the boundaries in the original data, for instance, using higher order derivatives [26,28]. Such computations can be integrated and performed efficiently on the graphics card. Alternately, segmentation of these datasets is also being considered, where we plan to take advantage of the 3D techniques in the Insight Segmentation and Registration Toolkit [29], or develop custom methods to DCE-MRI data. Finally, seamless integration with the medical informatics systems is also necessary, for use in a clinical environment.

Our breast tumor detection system is currently undergoing extensive testing at the Novant Health of Charlotte for evaluating its effectiveness. To date, we have investigated 168 'normal' breast cases and 188 abnormal cases, including 58 ductal invasive, 67 ductal carcinoma in situ, 39 lobular carcinoma, 3 inflammatory carcinoma cases and 21 mixed or anomalous cancer types. Future work will focus on using these clinical studies to discern the varying visual and temporal factors that will permit more robust classification to ascertain the degrees of specificity and sensitivity for this computational approach to detect various breast tumor lesions. Other work will focus on clinical studies involving a larger number of breast tumor cases that will permit more robust evaluation of specificity and sensitivity of breast tumor lesions across a number of attributes such as age, gender, prior treatment history.

References

[1] Morris EA, Liberman L, Balloon DJ, Robson M, Abramson AF, Heerdt A, et al. MRI of occult breast carcinoma in a high-risk population. Am J Roentgenol 2003;181(3):619–26.

[2] Liberman L, Morris EA, Benton CL, Abramson AF, Dershaw DD. Probably benign lesions at breast magnetic resonance imaging: preliminary experience in high-risk women. Cancer 2003;98(2):377–88.

[3] Morris EA. Screening for breast cancer with MRI. Semin Ultrasound CT MRI 2003;24(1):45–54.

[4] Kuhl CKK, Mielcareck P, Klaschik S, Leutner C, Wardelmann E, Gieseke J, et al. Dynamic breast mr imaging: are signal intensity time data useful for differential diagnosis of enhancing lesions? Radiology 1999;211(2):101–10.

[5] Mussurakis S, Buckley DL, Coady AM, Turnbull LW, Horsman A. Observer variability in the interpretation of contrast enhanced MRI of the breast. Br J Radiol 1996;69(827):1009–16.

[6] BI-RADS. Breast imaging reporting and data system atlas American College of Radiology. 2003, http://www.acr.org.

[7] Leach MO. Application of magnetic resonance imaging to angiogenesis in breast cancer. Breast Cancer Res 2001;3(1):22–7.

[8] Folkman J. The role of angiogenesis in tumor growth. Cancer Biol 1992;3:65–71.

[9] Boetes C, Barentsz JO, Mus RD, van der Sluis RF, van Erning LJ, Hendriks JH, et al. Mr characterization of suspicious breast lesions with a gadolinium-enhanced turboflash subtraction technique. Radiology 1994;193(3):777–81.

[10] Parker GJ, Suckling J, Tanner SF, Padhani AR, Revell PB, Husband JE, et al. Probing tumor microvascularity by measurement, analysis and display of contrast agent uptake kinetics. J Magn Reson Imaging 1997;7:564–74.

[11] Mussurakis S, Buckley DL, Drew PJ, Fox JN, Carleton PJ, Turnbull LW, et al. Dynamic mr imaging of the breast combined with analysis of contrast agent kinetics in the differentiation of primary breast tumours. Clin Radiol 1997;52(7):516–26.

[12] Elvins T. A survey of algorithms for volume visualization. Comput Graph 1992;26(3):40–7.

[13] Lorensen WE, Cline HE. Marching cubes: a high resolution 3d surface recon struction algorithm. Comput Graph 1987;21(4).

[14] Levoy M. Display of surfaces from volume data. IEEE Comput Graph Appl 1988;8(3).

[15] Drebin RA, Carpenter L, Hanrahan P. Volume rendering. Comput Graph 1988;22(4).

[16] Upson C, Keeler M. Vbuffer:visible volume rendering. Comput Graph 1988;22(4).

[17] Westover L. Footprint evaluation for volume rendering. Comput Graph 1990;24(4).

[18] Lacroute P, Levoy M. Fast volume rendering using a shear-warp factorization of the viewing transformation. 1998 symposium on volume visualization, p. 39–46; October 1998.

[19] Cabral B, Cam N, Foran J. Accelerated volume rendering and tomographic reconstruction using texture mapping hardware. 1994 symposium on volume visualization, p. 91–8; October 1994.

[20] Gelder AV, Kim K. Direct volume rendering with shading via three-dimensional textures. 1996 symposium on volume visualization, p. 23–30; October 1996.

[21] Lindholm E, Kilgard MJ, Moreton H. A user-programmable vertex engine. In: proceedings of ACM SIGGRAPH 2001, p. 149–58; 2001.

[22] Hadwiger M, Kniss JM, Engel K, Rezk-Salama C. High-quality volume graphics on consumer pc hardware. In: proceedings of SIGGRAPH 2002, course notes 42; August 2002.

[23] Mark WR, Glanville RS, Akeley K, Kilgard MJ. Cg: a system for programming graphics hardware in a c-like language. Comput Graph 2003;22(3). Proceedings of ACM SIGGRAPH 2003.

[24] Porter T, Duff T. Compositing digital images. Comput Graph 1984; 18(3):253–9.

[25] Spitzak B. The fast light toolkit. http://www.fltk.org.
[26] Kindlmann G, Durkin JW. Semi-automatic generation of transfer functions for direct volume rendering. In: IEEE symposium on volume visualization, p. 79–86; October 1998.
[27] Kniss J, Kindlmann G, Hansen C. Interactive volume rendering using multidimensional transfer functions and direct manipulation widgets for direct volume rendering. In: IEEE visualization, p. 255–62; October 2001.
[28] Kindlmann G, Whitaker R, Tasdizen T, Moller T. Curvature based transfer functions for direct volume rendering: methods and applications. In: IEEE visualization, p. 513–20; October 2003.
[29] Yoo TS, Ackerman MJ. A new program in medical image data processing. In: proceedings of the eigth annual medicine meets virtual reality (MMVR) conference, p. 385–91; 2000. http://visual.nlm.nih.gov/insight/.

Kalpathi R. Subramanian is an associate professor in the Department of Computer Science at the University of North Carolina at Charlotte. He obtained a BE (Honors) in Electronics and Communication Engineering from the University of Madras in 1983, followed by MS (1987) and PhD (1990) in Computer Science at the University of Texas at Austin. Between 1991 and 1993, he was a post-doctoral member of technical staff at AT&T Bell Laboratories in Murray Hill, New Jersey. He was an NIH Fellow during the summers of 2000 and 2001, at the National Library of Medicine. His research interests include scientific and information visualization, biomedical imaging and analysis, and design of interactive systems.

John P. Brockway is the President and Chief Executive Officer of Memory Testing Corporation, a medical research corporation. He received his PhD from the Pennsylvania State University in 1975, and has taught at the University of Konstanz, Germany, The Pennsylvania State University at University Park, Davidson College and is presently Adjunct Professor of Computer Science at the University of North Carolina at Charlotte. His principal research interests are functional magnetic resonance imaging (fMRI) and the detection and discrimination of mammographically and ultrasonically occult breast cancer.

William B. Carruthers received his BS degree in Computer Science in 2003, at the University of North Carolina at Charlotte, and is currently pursuing a Master's degree in Computer Science. His research interests include scientific visualization and medical image processing. From 2003 to 2004, he was the recipient of a student fellowship from the Novant Healthcare Foundation.